Changes in vascular density in resected tissue of 97 patients with mild malformation of cortical development, focal cortical dysplasia or TSC-related cortical tubers

Veersema, Tim J.; de Neef, Andrew; van Scheppingen, Jackelien; Ferrier, Cyrille H.; van Eijsden, Pieter; Gosselaar, Peter H.; van Rijen, Peter C.; Spliet, Wim G. M.; Braun, Kees P. J.; Mühlebner, Angelika; Aronica, Eleonora

Published in:
International journal of developmental neuroscience

DOI:
10.1016/j.ijdevneu.2019.11.003

Published: 01/01/2019

Document Version
Publisher's PDF, also known as Version of record

Citation for pulished version (APA):
Veersema, T. J., de Neef, A., van Scheppingen, J., Ferrier, C. H., van Eijsden, P., Gosselaar, P. H., van Rijen, P. C., Spliet, W. G. M., Braun, K. P. J., Mühlebner, A., & Aronica, E. (2019). Changes in vascular density in resected tissue of 97 patients with mild malformation of cortical development, focal cortical dysplasia or TSC-related cortical tubers. *International journal of developmental neuroscience*, *79*, 96-104. https://doi.org/10.1016/j.ijdevneu.2019.11.003

International Journal of Developmental Neuroscience 79 (2019) 96–104

Contents lists available at ScienceDirect

International Journal of Developmental Neuroscience

journal homepage: www.elsevier.com/locate/ijdevneu

Changes in vascular density in resected tissue of 97 patients with mild malformation of cortical development, focal cortical dysplasia or TSC-related cortical tubers

Tim J. Veersema[a,1], Andrew de Neef[b,1], Jackelien van Scheppingen[b], Cyrille H. Ferrier[a], Pieter van Eijsden[a], Peter H. Gosselaar[a], Peter C. van Rijen[a], Wim G.M. Spliet[c], Kees P.J. Braun[a], Angelika Mühlebner[b,*,2], Eleonora Aronica[b,d,2]

[a] Department of Neurology and Neurosurgery, UMC Utrecht Brain Center, University Medical Center Utrecht, Utrecht, the Netherlands
[b] Department of (Neuro) Pathology, Amsterdam UMC, University of Amsterdam, Amsterdam, the Netherlands
[c] Department of Pathology, University Medical Center Utrecht, Utrecht, the Netherlands
[d] Stichting Epilepsie Instellingen Nederland (SEIN), the Netherlands

ARTICLE INFO

Keywords:
Refractory epilepsy
Epilepsy surgery
Mild malformation of cortical development
Focal cortical dysplasia
Tuberous sclerosis complex
Vascular density

ABSTRACT

Recent studies suggested a possible association between malformations of cortical development and microvascular density. In this study we aimed to further elucidate the relation between microvascular density and cortical developmental abnormalities in a cohort of 97 patients with epilepsy and histologically proven mild malformation of cortical development (mMCD), focal cortical dysplasia (FCD) or tuberous sclerosis complex (TSC). Surgical tissue samples were analyzed with quantitative measures of vessel density, T-cell response, microglial activation and myelin content. Subsequently, the results were compared to an age- and localization matched control group. We observed an increase in microvasculature in white matter of TSC cortical tubers, which is linked to inflammatory response. No increase was seen in mMCD or FCD subtypes compared to controls. In mMCD/FCD and tubers, lesional cortex and white matter showed increased vascular density compared to perilesional tissues. Moreover, cortical vessel density increased with longer epilepsy duration and older age at surgery while in controls it decreased with age. Our findings suggest for that the increase in white matter vascular density might be pathology-specific rather than a consequence of ongoing epileptic activity. Increased cortical vessel density with age and with longer epilepsy duration in mMCD/FCD's and tubers, however, could be a consequence of seizures.

1. Introduction

Epilepsy in young people is often caused by malformations of cortical development (Blumcke et al., 2017), some of which are focal in nature and therefore termed focal cortical dysplasia (FCD). The International League Against Epilepsy (ILAE) published a new classification system for FCD which acknowledges three subtypes of FCD (Blümcke et al., 2011). Type I is characterized by abnormal cortical layering, either by persistent radial micro-columnar architecture (Ia) or by a disruption of the horizontal lamination (Ib) or both (Ic). Type II is characterized by severe disorganization of the cortex and dysmorphic neurons (IIa), and balloon cells in addition (IIb). FCD type III refers to FCD in combination with other pathologies, such as hippocampal sclerosis (FCD type IIIa), glial or glioneuronal tumors (FCD type IIIb), vascular malformations (FCD type IIIc) or any other principal lesion acquired during early life (FCD type IIId). The most subtle architectural abnormalities in the FCD spectrum are classified as mild malformations of cortical development (mMCD), characterized by excessive number of

Abbreviations: BBB, Blood Brain Barrier; ILAE, International League Against Epilepsy; FCD, Focal cortical dysplasia; (m)MCD, (mild) Malformation of cortical development; TSC, Tuberous Sclerosis Complex; ROI, Region of Interest; MANCOVA, Multivariate analysis of covariance; ASL-MRI, Arterial spin labelling magnetic resonance imaging; SPECT, Single-photon emission computed tomography; FDG-PET, fluorodeoxyglucose positron emission tomography; VEGF, Vascular endothelial growth factor; GI, grey intensity value

* Corresponding author at: Department of (Neuro) Pathology, Amsterdam UMC, University of Amsterdam, Meibergdreef 9, 1105 AZ Amsterdam, the Netherlands.
E-mail address: a.muehlebnerfahrngruber@amc.nl (A. Mühlebner).
[1] Contributed equally to this manuscript.
[2] Shared senior author.

https://doi.org/10.1016/j.ijdevneu.2019.11.003
Received 18 February 2019; Received in revised form 13 October 2019; Accepted 22 November 2019
Available online 23 November 2019

neurons in the molecular layer (type 1) or white matter (type 2) without the presence of any other structural abnormalities – in contrast to FCD I types and II types (Blümcke et al., 2011; Palmini et al., 2004). mMCD as separate entity is subject to debate, but was included in the FCD ILAE classification, albeit as addendum (Blümcke et al., 2011). Our group's recent surgical cohort study demonstrated differences between patients with mMCD and FCD histological diagnoses in clinical presentation and surgical outcome, in support of this clinical differentiation (Veersema et al., 2019).

A syndrome associated with refractory epilepsy that begins often in early childhood is Tuberous Sclerosis Complex (TSC). TSC is a genetic disorder caused by mutations in either the *TSC1* or *TSC2* gene expressed as hamartomas or benign tumors in several organ systems (Aronica and Mühlebner, 2017; Curatolo et al., 2018). In the brain TSC can cause subependymal nodules, subependymal giant cell astrocytomas and cortical tubers which are typically associated with seizures. Tubers found in TSC are histologically often indistinguishable from FCD type IIb (Blümcke et al., 2011). Calcifications may differentiate tubers from FCD, but since over two-thirds do not exhibit this stigma, it is not a reliable distinguishing feature (Mühlebner et al., 2016).

In both isolated mMCD/FCD of all types, and in TSC, surgical removal of the epileptogenic lesion can result in seizure freedom (Blumcke et al., 2017; Liang et al., 2017). Because many of these lesions are difficult to spot or outline on conventional MRI, or multiple in nature, it is often difficult to determine in which patients surgery is indicated. Therefore, it is of clinical importance to investigate associations between radiological features of FCD, histological characteristics and clinical outcomes. Recently 7 T MR imaging suggested a possible association between FCD and microvascular density (De Ciantis et al., 2015; Veersema et al., 2016), which could possibly be used as diagnostic marker for dysplastic lesions. Evidence for increased vasculature in FCD lesions was found by Wintermark et al. using quantitative histological techniques and Arterial spin labelling (ASL)-MRI (Wintermark et al., 2013). In contrast, Blauwblomme et al. found disorganized vascular structure but no increased density, and in their study PET-CT and ASL-MRI suggested lesional hypo- rather than hyperperfusion (Blauwblomme et al., 2014). ASL MRI showed hypo and hyperfused tubers in patients with tuberous sclerosis, and while it was uncertain if hyperperfusion reflected epileptogenicity, a larger number of hyperperfused tubers in a patient was associated with increased seizure frequency (Pollock et al., 2009).

Uncertainty remains whether there is true increased vascular density in FCD or tubers, and if these changes would be an intrinsic etiological factor of epileptogenesis, part of the underlying malformation, or a result of aberrant neuronal activity. In this study we aimed to further elucidate the relation between microvascular density and cortical developmental abnormalities in a cohort of patients with histologically proven mMCD/FCD or TSC, and with possible etiopathological factors.

2. Material & methods

All patients who underwent epilepsy surgery between 2000 and 2012 at the University Medical Center Utrecht and had an initial histopathological report compatible with current mMCD/FCD subtypes were included. The pathological diagnosis was reviewed and established according to the currently available classification schemes for lesions associated with therapy-refractory epilepsy (Blümcke et al., 2011; Palmini et al., 2004). Patients with complex malformations (e.g. polymicrogyria, hemimegalencephaly) and associated cortical dysplasia (FCD III types) were omitted from the study.

Cortical tuber samples were added to the cohort by selecting patients from the database operated between 2002 and 2013 with confirmation of TSC through genetic testing and of whom tissues samples were available after resective epilepsy surgery. In addition to TSC gene defects, (combinations of) multiple cortical or subependymal abnormalities, cutaneous stigmata or typical abnormalities in kidneys, heart or lung lead to a clinical TSC diagnosis, following the standard diagnostic criteria for TSC (Northrup and Krueger, 2013).

The age- and localization-matched control group consisted of 14 autopsy cases. None of these patients had a history of seizures or other neurological diseases. All control samples were collected at the Department of (Neuro) Pathology, AMC, Amsterdam, The Netherlands.

Tissue was obtained and used in accordance with the Declaration of Helsinki and the AMC Research Code provided by the Medical Ethics Committee and approved by the science committee of the UMC Utrecht Biobank.

2.1. Tissue preparation and immunohistochemistry

The tissue was carefully oriented, cut perpendicular to the pial surface, fixed overnight in 4 % formaldehyde and routinely processed into liquid paraffin. Sections were cut at 4 − 6 μm with a microtome (Microm, Heidelberg, Germany), and mounted on positively charged slides (Superfrost + Menzel, Germany). Each specimen was histopathologically examined using hematoxylin & eosin (H & E). The revised diagnosis was based on following commonly used immunohistochemical stainings: NeuN, SMI32, Vimentin, GFAP, and MAP2. The tissue samples were reclassified according to the 2011 ILAE classification system. Additional stainings were performed when necessary.

The immunohistochemical examinations for the quantitative analysis of all surgical specimens was performed using the following antibodies: CD34 (cluster of differentiation 34, 1:600, Qbend, Immunotech) endothelial staining for vascular density, CD3 (cluster of differentiation 3, 1:200, clone F7.2.38, DAKO) for T-cell presence, Cr3/43 (HLA - DP, DQ, DR antigen, DAKO) for microglia activation, GFAP (glial fibrillary acid protein, 1:4000, Dako, Glostrup, Denmark) for gliosis, MBP (myelin binding protein, 1:400 DAKO) for myelinization, NeuN (neuronal nuclei 1:100, clone A60, Chemicon, Billerica, MA, USA) for neurons, non-phosphorylated neurofilament H (SMI32) (1:1000, clone SMI32, Sternberger, Lutherville). The semi-quantitative analysis of blood brain barrier disruption was performed using albumin staining (Albumin Rabbit polyclonal 1:20,000 DAKO, Glostrup, Denmark). The slides were air dried overnight at 37 °C. All immunohistochemical stainings were performed with a Ventana semi-automated staining machine (Benchmark ULTRA; Ventana, Illkirch, France) and the Ventana DAB staining system according to the manufacturer's protocol.

2.2. Quantitative measurements

The CD34 stained slides were digitized using an IntelliSite Ultra Fast Scanner (Phillips healthcare Best, the Netherlands). Other stainings were digitized with an Olympus dotSlide system (vs 2.5, Olympus, Tokyo, Japan). In both scanners the magnification size was set on 100x and pixels size was 0,64 μm^2. The slides were converted to Tagged Image File Format (TIFF) files. Every file was subsequently divided into evenly spread tiles. In Photoshop (Version: 2015.1.2) regions of interest (ROI's) with a median size of 0.83 mm^2 (range: 0.23–6.5 mm^2) were selected for the analysis. The selected ROI's were evenly spread within cortex, subcortical white matter (white matter was defined as being > 500 μm away from the grey white matter border), lesion and, when available, perilesional tissue. Perilesional tissue was defined by the absence of aberrant cell forms such as dysmorphic neurons and balloon/ giant cells (for FCD II or TSC) and by normal cortical architecture (FCD subtypes and TSC). The lesional border in mMCD is less obvious, due to the subtle characteristics; perilesional tissue shows no excessive neurons in layer 1 or white matter.

The available images were color deconvoluted according to the following RGB values: red: 0.26814753, green: 0.57031375 and blue: 0.77642715. The resulting 8bit image was converted to a black and white mask (black: positively stained area, white: no staining). To

Table 1
Patient characteristics.

Diagnosis	Number of patients	Gender ♂ / ♀	median age at surgery yrs. (range)	Localization tissue samples F	T	P	O	Lesional[a]	Perilesional[a]	median epilepsy duration yrs. (range)
mMCD	31	13 / 18	23 (1–48)	9	17	4	1	32	0	10 (1–32)
mMCD type 1	7	3 / 4	32 (19–48)	4	3	0	0	8	0	16 (7–32)
mMCD type 2	24	10 / 14	19 (1–46)	5	14	4	1	24	0	7 (1–30)
FCD I	9	3 / 6	13 (7 months – 56 yrs.)	3	5	1	0	9	1	5 (1–42)
FCD Ia	4	2 / 2	2 (7 months – 56 yrs.	0	3	1	0	4	0	2 (1–42)
FCD Ib	4	1 / 3	14 (5–40)	2	2	0	0	4	1	7.5 (2–23)
FCD Ic	1	0 / 1	32	1	0	0	0	1	0	23
FCD II	44	25 / 19	13 (3 months – 46)	32	7	4	1	46	3	7.5 (0–37)
FCD IIa	17	11 / 6	13 (3 months-45 yrs.)	12	4	1	0	18	1	6 (0–37)
FCD IIb	27	14 / 13	13 (8 months-41 yrs.)	20	3	3	1	28	2	9 (1–36)
TSC	13	7 / 6	9 (10 months-47	9	4	0	0	14	3	5 (1–35)
total	97	48 / 49	14 (3months-56 yrs.	53	33	9	2	101	7	8 (0–42)

Overview of the patients, gender distribution (♂ = male, ♀ = female) lesion type and location, epilepsy duration in years. The different pathology types are mild malformation of cortical development (mMCD), Focal cortical dysplasia (FCD) and Tuberous Sclerosis Complex (TSC). The different brain regions are Frontal (F), Temporal (T), Parietal (P), Occipital (O). [a] Note, for certain patients only lesional, perilesional tissue or both were available for analysis. The sum of lesional and perilesional samples exceeds the number of patients due to three patients that underwent surgery twice and seven patients with both lesional and perilesional samples available for analyses.

discard background noise, a grey intensity value (GI) for each individual stain was selected.

2.3. Quantitative analysis of cells and microvasculature

To improve the accuracy and to avoid counting vessels or cells multiple times, a size range in μm^2 was selected for each staining and no watershed filter was used. Microvessel count was performed using CD34 (GI: 210, Pixel: 30-unlimited μm^2), including capillaries and parenchymal arterioles. For the count of inflammatory cells, CD3 was used (GI: 160, Pixel: 10-unlimited μm^2). Neuronal cell bodies were counted with NeuN (GI: 180, Pixel: 30-unlimited μm^2). To analyze the amount of dysmorphic neuron, SMI32 was used (GI: 50, Pixel: 100-unlimited). All images were automatically processed via FIJI (ImageJ2, v64, open source) with a specifically developed macro based on Java programming language. Semi-automated quantification methods have been validated in our lab and described previously (Scholl et al., 2017).

Initial analysis revealed differences in vascular densities between tubers and controls that prompted further analysis of potential additional and explanatory contrasts or relationships regarding neuroinflammation, blood brain barrier dysfunction, and myelin content in tubers.

2.4. Quantitative analysis of area size

For area size analysis the total area of the ROI was determined using Image J. Subsequently the GI was set to remove background noise. Finally, field fraction of positively stained area was calculated. CR3/43 was used to measure microglial activation. To determine the number of reactive astrocytes, GFAP was used. Myelin content was examined using MBP. The GI for all area size stainings was set on 180. The images were processed with a specific macro-based field fraction Java programming language in FIJI.

2.5. Semi-quantitative scoring of balloon/giant cells and blood brain barrier damage

The number of balloon/giant cells was scored on high power fields using an Olympus BX 50 microscope (each representing $1.081 mm^2$). The area of highest density was taken into account. We assessed the total coverage of abnormal cells within the grid area resulting in the following scores: I: 0–25 %, II: 25–50 %, III: 50–75 % and IV: 75–100 %. Blood brain barrier damage was also analyzed according to the same technique as used in earlier studies (Aronica et al., 2012; Englot et al., 2012; Prabowo et al., 2013). The intensity of the albumin staining was scored using a semi-quantitative scale ranging from 0 to 3 (0: negative, 1: weak, 2: moderate, 3: strong reactivity).

Quantitative and automated methods were not suitable for scoring balloon/giant cells or albumin extravasation due to non-specific staining patterns.

2.6. Clinical data

Clinical patient data was collected for age at surgery, seizure duration in years and location of resected tissue (frontal, temporal, parietal or occipital).

2.7. Statistical analysis

Statistical analysis was performed with SPSS version 22 and 25 (IBM, PASW Statistics, USA). Descriptive statistics were used for the primary analysis: counts, mean, standard deviation. Vascular density counts were tested for normal distribution using Shapiro-Wilk test and for homogeneity of variances (scatterplot predicted versus observed). Test for normality (Shapiro-Wilk, $p < 0.001$) and homogeneity of variances (scatterplot predicted versus observed for vascular density and age) – failed for white matter vascular density. Therefore, we performed a natural logarithmic transformation for white matter vascular density. Grey matter and the log-transformed white matter vascular density showed normal distribution and homoscedasticity. *T*-test was used to assess differences in vascular densities between sex. We used multivariate analysis of covariance (MANCOVA) to test dependence of grey and white matter vascular density on age, region, epilepsy duration and consequently for differences between pathologies and for groupwise comparison of lesional versus perilesional densities. Multiple testing in post-hoc analysis was corrected for with Hochberg or Dunnett's test because of differences in sample sizes. Correlation was tested with Pearson's test, Kendell-Tau for correlation with semi-quantified balloon cell density and Spearman's rho for semi-quantifications of albumin leakage. Paired-T test was performed to assess lesional versus perilesional vessel densities within the same patients.

3. Results

Patient characteristics are summarized in Table 1. In total 97 patients with either mMCD, FCD or TSC were included (31 mMCD, 52 FCD, 13 TSC). Median age at surgery was 14 years (range 3 months – 56 years). Three patients with FCD underwent a second surgical resection

Table 2
Vascular densities in cortex and white matter.

	vascular density in cortex, count/mm^2				vascular density in white matter, count/mm^2			
	mean ± SD	median	range	p	mean ± SD	median	range	p
controls	154.3 ± 40.8	154.1	73.7-237.2	0.057[a]	69.1 ± 17.4	65.2	44.6-118.3	0.866[a]
Lesional	147.2 ± 44.4	142.3	5.51 – 277.4		76.3 ± 51.1	62.8	32.2-348.7	
perilesional	116.7 ± 39.4	99.0	73.7-192.0		69.0 ± 23.3	65.8	41.4–99.2	
frontal (controls)	168.9 ± 16.8	164.7	154.3-191.8	0.03[b]	65.6 ± 10.5	66.8	51.7-76.9	0.579[b]
temporal (controls	130.4 ± 29.2	133.1	73.7-166.3		66.0 ± 11.7	65.1	44.6-80.5	
parietal (controls)	–	–	–		–	–	–	
occipital (controls)	221.0 ± 23.0	204.7	204.7-237.2		88.6 ± 42.0	88.6	58.9-118.3	
frontal (lesional)	162.2 ± 40.4	167.4	71.0-233.1	< 0.0005[b]	84.2 ± 56.9	67.7	32.2-348.7	0.224[b]
temporal (lesional)	124.5 ± 43.8	123.2	5.3-277.4		67.2 ± 48.6	56.3	32.4-325.3	
parietal (lesional)	140.8 ± 28.5	142.3	81.2-181.7		66.9 ± 16.7	62.1	48.5-106.5	
occipital (lesional)	184.6 ± 57.0	184.6	144.3-224.9		54.0 ± 5.0	54.0	50.5-57.6	
mMCD (lesional)	145.1 ± 39.6	139.0	55.3-233.1	0.495[a]	57.0 ± 12.7	56.2	32.2-81.8	< 0.0005[a]
FCD I (lesional)	143.2 ± 41.7	135.2	89.0-220.6		59.5 ± 8.3	61.8	44.8-71.1	
FCD IIa (lesional)	153.3 ± 58.3	168.2	5.3-231.0		60.7 ± 11.3	62.4	35.6-77.2	
FCD IIb (lesional)	149.5 ± 30.9	151.4	96.3-221.7		73.6 ± 11.3	62.4	35.6-77.2	
TSC	143.0 ± 59.1	131.3	52.5-277.4		146.2 ± 98.2	106.8	41.3-348.7	

[a] Mancova, corrected for age and region.
[b] Mancova, corrected for age mMCD: malformation of cortical development. FCD: focal cortical dysplasia. TSC: tuberous sclerosis complex.

because of recurrent seizures.

3.1. Control tissue vessel density

As control group we included 14 cortical post-mortem samples (median age 15 years, range 2–42), sex: 9 male; location: 4 frontal, 8 temporal, 2 occipital). For 7 patients perilesional samples were also available (1 FCD Ib, 1 FCD IIa, 2 FCD IIb and 3 TSC). "Perilesional" was defined as cortex surrounding a main FCD II or TSC lesion without presence of giant cells or dysmorphic neurons. Subtle cortical abnormalities may be present. The group size of all pathologies included was highly variable, therefore we fused the groups into mMCD (n = 31), FCD I (n = 10), FCD IIa (n = 18), FCD IIb (n = 28) and TSC (n = 13). Quantifications of vascular density are provided in Table 2.

In post-mortem control tissue we measured a mean vascular density of 154.3 ± 40.8/mm^2 in cortex and in white matter a median density of 65.2/mm^2 (range 44.6–118.3). To further characterize vascular density in controls, we first compared vascular density between men and women and found no significant differences in cortex (t(12) = 1.026, p = 0.325), or white matter (t(12) = 1.346, p = 0.195). White matter and cortical vascular density were correlated (r = 0.551; p = 0.041). In multivariate regression analysis we found a significant association between vascular densities and age (F(2,9) = 5,252; p = 0.031; Wilk's λ = 0.461) and brain region (F(4,18) = 3.988; p = 0.017; Wilk's λ = 0.280). Corrected for region, there was a negative association between age and cortical vessel density (F(1) = 11.512; p = 0.007; r(14) = −.704, p = 0.005) (Figs. 1 and 2**a**) but not between age and white matter vessel density (F(1) = 2.289; p = 0.161,) (Figs. 1 and 2**c**). There was a significant effect of region on cortical vascular density for cortex (F(2) = 11.024, p = 0.03), correcting for age. Occipital regions (221.0 ± 23.0/mm^2) had highest cortical vascular density followed by frontal (168.9 ± 16.8 /mm^2) and temporal regions (130.4 ± 29.2/mm^2) (no parietal control samples).

3.2. Patient tissue vessel density

In the analysis of vascular density in lesional tissue of 97 patients no sex difference was detected either (cortex *t*-test p = 0.771; white matter *t*-test p = 0.917). Corrected for age, there were significant regional differences in cortex (F(3) = 8.021, p < 0.0005) but not in white matter (F(3) = 1.482, p = 0.224) vascular density. Highest cortical vascular density was found occipitally (mean 184.57 ± 57.02 vessels per mm^2), followed by frontal lobe (mean 162.24 ± 40.36), parietal lobe (mean 147.41 ± 20.53) and temporal lobe cortex (mean 122.53 ± 43.60). In post-hoc analysis – omitting age as co-variate - there were significant differences between frontal and temporal (LSD, p < 0.0005, Hochberg p < 0.0005) and between temporal and occipital lobe cortical vascular densities (LSD, p = 0.041, Hochberg = 0.220).

Corrected for region, vessel density in lesional samples was positively associated with age at surgery (F(2,93) = 7.163 p = 0,001) and with epilepsy duration (F(2,93) = 5.400, p = 0.006) in cortex (Fig. 2**a**,**b**), but not in white matter (Fig. 2**c**,**d**). The positive relation between age and cortical vascular density was more pronounced in TSC (Fig. 2**b**).

Corrected for age and region we found no significant vascular density differences in groupwise comparison between lesional samples

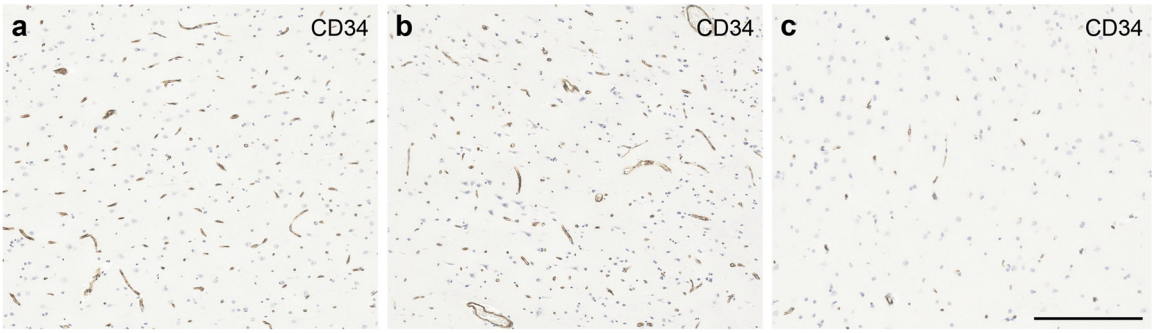

Fig. 1. Cortical vascular density in healthy controls declines with age, p = 0,007. The temporal region of a 2-year-old (**a**), 17-year-old (**b**) and 42-year-old subject (**c**) *scale bar* in d = 100 μm.

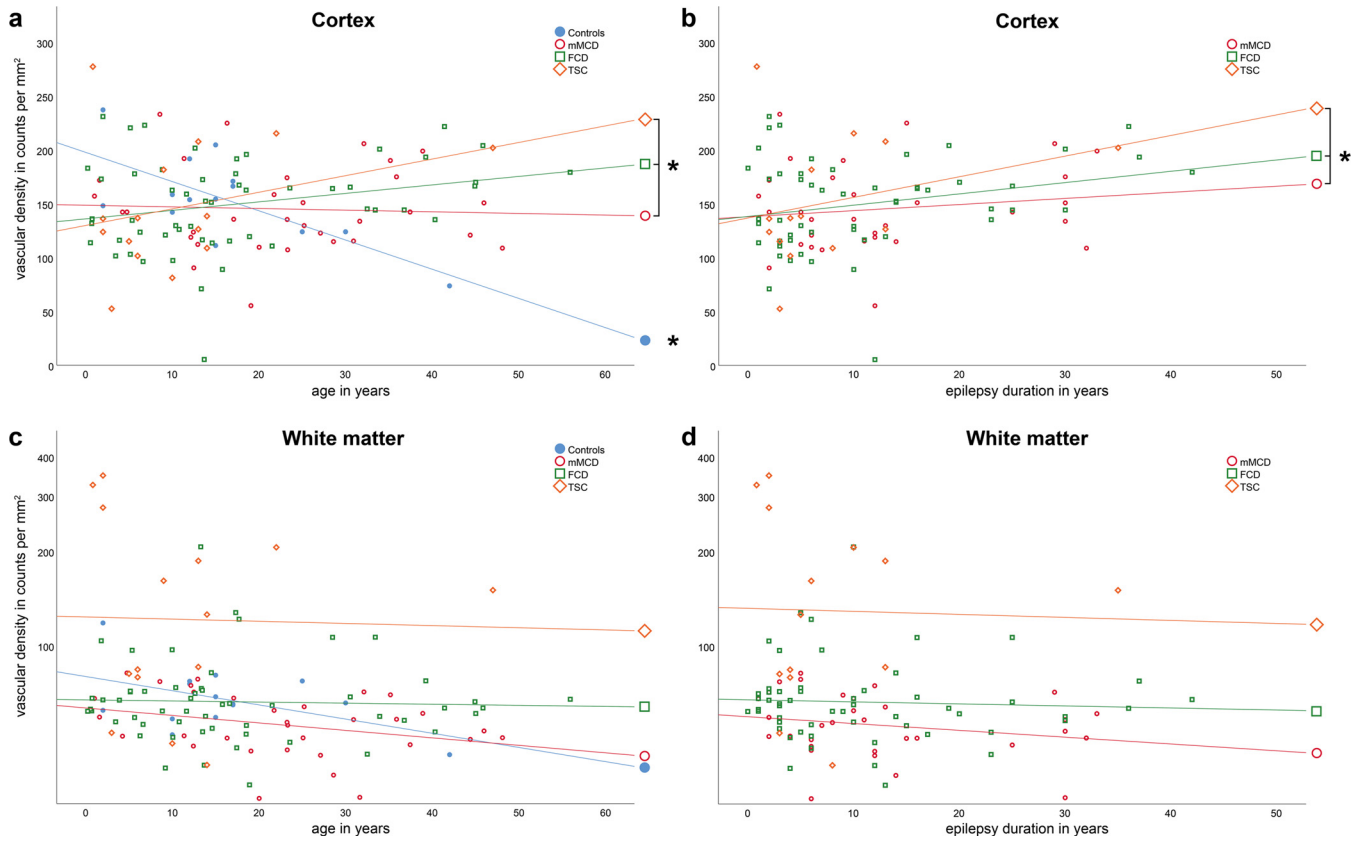

Fig. 2. Vascular density in cortex (**a,b**) and white matter (**c,d**) in controls, mMCD, FCD and TSC samples in relation to age at surgery (**a,c**) and epilepsy duration (**b,d**). There is no relation between age and epilepsy duration and vascular density in white matter (**c,d**), while in cortex density declined with age in controls (a) and increased with age and epilepsy duration in lesions, most pronounced in TSC (**b,d**).

and controls ($F(2,104) = 0.982$, $p = 0.399$, Wilk's $\lambda = 0.928$).

Groupwise comparison between lesional (147.2 ± 44.4 /mm^2) and perilesional (116.7 ± 39.4 /mm$^{2)}$ cortical density showed a trend for higher density of lesional tissues, regardless of age and region ($F(1) = 4.025$, $p = 0.048$). No difference was found in white matter vascular densities ($F(1) = 0.152$, $p = 0.698$).

In a pairwise analysis of the 7 patients of whom both lesional and perilesional samples were available we found significantly higher vascular densities in the lesional cortex ($t(6) = 3.156$, $p = 0.02$) (Fig. 3**a**) and in the lesional white matter ($t(6) = 2.733$, $p = 0.034$) (Fig. 3**d**) compared to perilesional tissue (lesional cortex 160.2 ± 30.4, perilesional cortex 116.7 ± 39.4 /mm^2; lesional white matter median 96.7, range 52.9–206.0, perilesional white matter median 65.8 range 41.4–99.2 /mm^2). In all individual cases lesional cortex had a higher vascular density than the neighboring perilesional tissue. In 5 of 7 white matter pairs, vascular density was higher in the lesional tissue.

We compared vessel densities between the different pathologies with grouping of mMCD (type 1 and 2), FCD I (a, b and c), FCD IIa, FCD IIb and cortical tubers in TSC. Corrected for age and region there were significant differences between pathologies in lesional vascular density ($F(10,184) = 5.478$, $p < 0.005$, Wilk's $\lambda = 0.594$). This is due to significant differences in white matter vessel densities across pathologies ($F(5) = 9.569$, $p < 0.0005$). No differences were found in cortical density ($F(5) = 0.884$, $p = 0.495$). Post-hoc testing showed that only TSC samples (median 106.8, range 41.3-348.7 mm^2) had a significantly higher white matter vascular density compared to control samples (median 65.2, range 44.6-118.3 mm^2, Dunnett, $p < 0.0005$) (Fig. 4**a**). Perilesional samples were excluded from these analyses.

There was no correlation between balloon cell density and vessels in FCD IIb and TSC (Kendall-tau, grey matter $p = 0.679$, white matter $p = 0.196$).

FCD IIb and cortical tubers have identical histological features. However, we observed a difference in white matter vascular density between FCD IIb and tubers. Corrected for age, white matter vascular density was significantly different ($F(2,36) = 9.683$, $p < 0.0005$, Wilk's $\lambda = 0.650$), with higher densities in TSC (median 106.8 range 41.3–348.7 mm2) compared to FCD IIb (median 62.4, range 35.6–77.2) (F1) = 16.481 $p < 0.0005$;). Cortical vessel density did not differ between FCD IIb and tubers.

Because cortical tubers of the TSC cohort showed a significantly higher number of vessels in white matter compared to controls, we continued to examine the tuber samples with different stainings which were mainly focused on the role of inflammation and the damage of the blood brain barrier (BBB). Because of the lack of differences between the FCD and control groups, we did not examine more stainings within FCD or mMCD groups.

TSC samples showed a positive correlation between vascular density in white matter and microglial activation (Cr3/43 positivity, $r(10) = 0.716$, $p = 0.02$) (Fig. 4**e**).

White matter vascular density tended to correlate with inflammatory cell response (CD3 activity, $r(10) = 0.563$, $p = 0.09$). Inflammatory cell response significantly correlated with microglial activation in white matter ($r(10) = 0.823$, $p = 0.003$). We did not find a correlation between vascular density and myelin content.

We then performed a semi-quantitative analysis of the BBB leakage, with albumin as marker. Albumin deposits were observed in grey and white matter in all TSC samples (Fig. 5), but there was no significant correlation between quantities of extracellular albumin and vascular density.

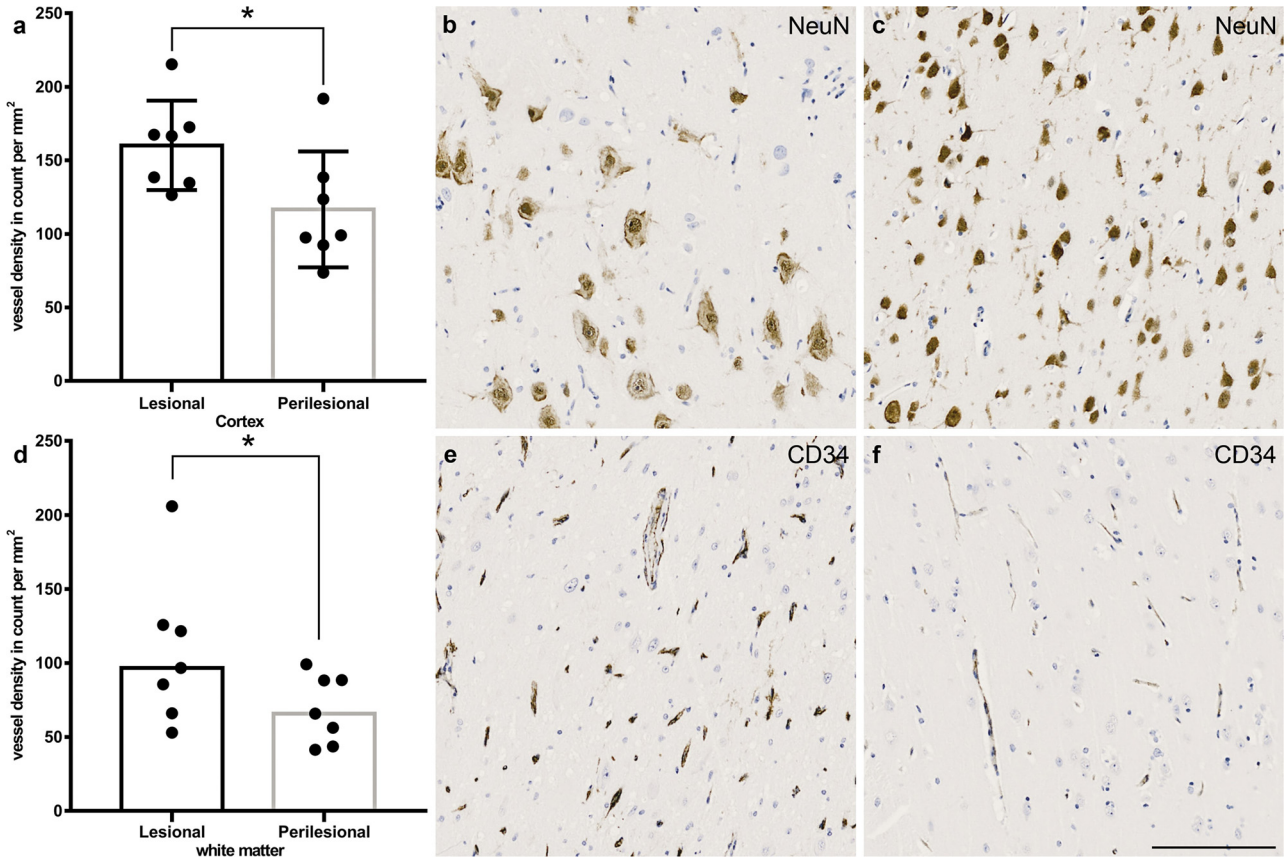

Fig. 3. Lesional vs perilesional vascular densities in cortex (**a**) and white matter (**d**). Significant difference in vessel density (per mm^2) in pairwise analysis between lesional and perilesional grey matter ($p = 0.02$) (**a**, mean and 1 std for bar and whiskers), and white matter ($p = 0.034$) (**d**, median for bar, non-parametric data). A characteristic feature of type IIb focal cortical dysplasia is the presence of dysmorphic neurons (**b**) (as shown by NeuN staining, in grey matter). Perilesional grey matter (**c**) does not contain dysmorphic neurons. Lesional vessel density in FCD IIb (**e**) (as shown by CD34 staining) compared to perilesional vessel density (**f**) in grey matter. *Scale bar* in $f = 100$ μm and also applies to **b**, **c**, **e**, **f.**

4. Discussion

This study provides the first description of relationship between microvascular density and cortical developmental abnormalities in a large cohort of patients with either cortical dysplasia or cortical tubers in TSC.

We found that cortical and white matter vascular density is increased in FCD and tubers compared to the surrounding perilesional cortex, irrespective of age. While in healthy controls cortical vascular density decreased with age, in epilepsy patients with FCD or tubers density appeared to increase with age and with longer epilepsy duration. No time-relation was seen in white matter vascular density. Tubers had an increased microvascular density in white matter compared to age-matched controls. The latter was associated with microglial activation and an increased number of inflammatory cells.

In both healthy subjects and in patients there were significant regional differences in cortical vascular density. The highest densities were found in the occipital region, followed by frontal, parietal and temporal locations. This is likely linked to the regional differences in brain metabolism (Ishi et al., 1996; Wong-Riley, 2010). Moreover, several studies have indicated that the same area consists of a higher numbers of neurons which are necessary for the visual processing (Collins et al., 2010; Rockel et al., 1980; Skoglund et al., 1996; Young et al., 2013). However, the high level of variance amongst the existing studies does not allow clear-cut conclusions concerning topography of vascular density. As described by Riddle et al., a more robust analysis of the different regions in the brain, with a standardized method is needed, to see if this finding is consistent in the general population (Riddle et al., 2003).

Furthermore, our data suggests not only differences in vascular density between brain regions, but also variation with age due to constant remodeling of the brain, a process thought to be mainly based on the functional needs of the brain (Marín-Padilla, 2012; Mito et al., 1991).

Although there is not yet a clear consensus on the effect of age on vascular density, a decline has been observed in several studies (Riddle et al., 2003). Correspondingly, we found a decrease in cortical vascular density with advancing age in controls.

In contrast to normal cortex, in resected malformations of cortical development – most pronounced in cortical tuber – we observed an increase in vascular density with ageing. This could suggest that certain processes in lesional or epileptogenic cortex drive ongoing angiogenesis and increasing vascularity, rather than that the higher vessel density is static and reflects and intrinsic part of the developmental abnormality. Moreover, in contrast to cortical vascular density, vessel density in white matter was related to pathology specific processes. Compared to controls, increased density was only observed in tubers and not in FCD subtypes.

We did not perform rater variability analysis for the mMCD/FCD reclassification, but prior research has shown good intra-observer reliability, good interobserver agreement for FCD II subtypes and moderate agreement for non-FCD and FCD Ia en Ib types in the evaluation according to the 2011 ILAE classification (Coras et al., 2012). However, we acknowledge that no such attempt has been made for the mMCD so far and therefore this group remains rather heterogeneous, albeit with distinct clinical features (Veersema et al., 2019).

During brain development, early migration in particular, neuronal progenitor cells associate with blood vessels of the vascular plexus in

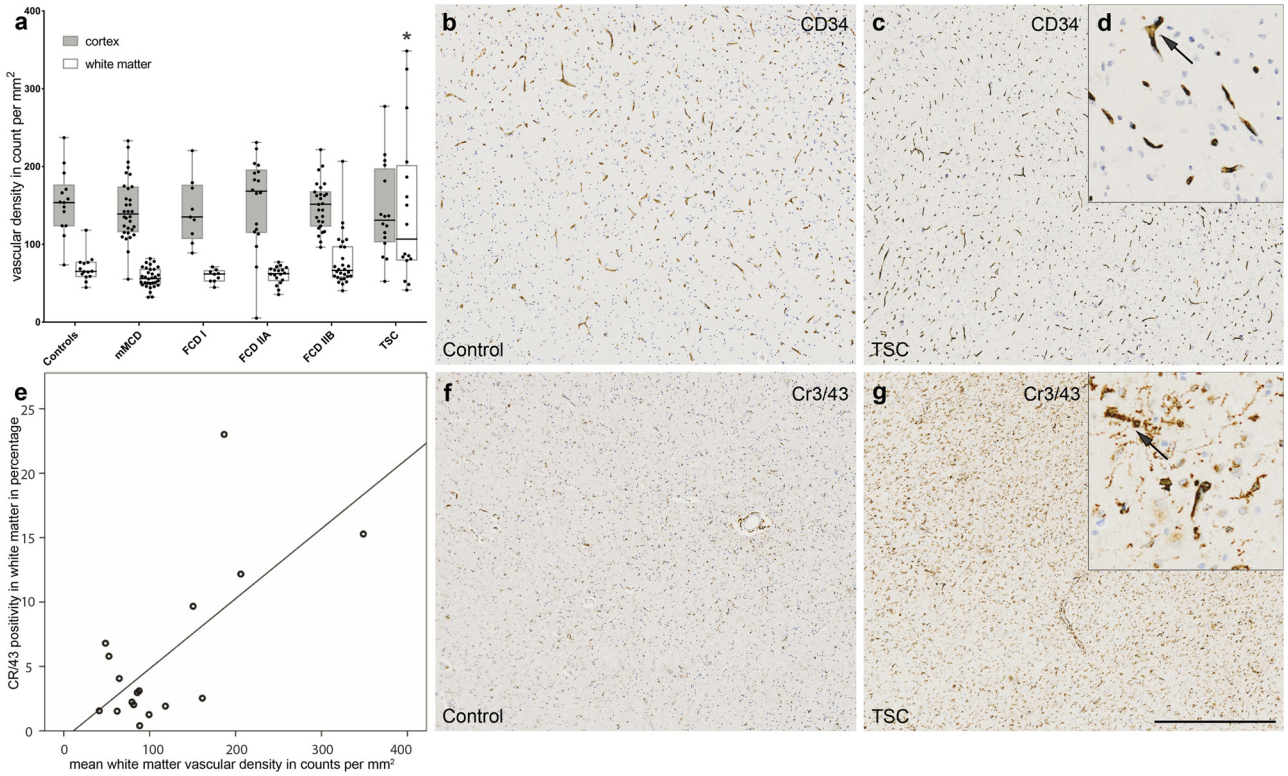

Fig. 4. Histological subgroups, vascular density and microglia activation. **a** Increased white matter vessel density in TSC compared to control in white matter, $p < 0.001$ (box shows median and 25th and 75th percentile, whiskers min-max). Vessel density in white matter in a healthy control (**b**) and a cortical tuber in a patient with TSC (**c**). micro-vasculature is clearly visible with CD34 endothelial staining (**d**). increased vessel density is accompanied with increased microglia activation in a tuber (**e**), $p < 0.05$. Microglial activation in control (**f**) vs TSC (**g**). Microglial activation can clearly be seen with Cr3/43 staining (**h**). *Scale bar* in g = 100 μm and also applies to **b–c** and **f–g**.

the (sub)ventricular zone - which develops relatively early in embryogenesis, - and migrate abluminally to their target location in the cortex. This vasophilic migration mechanism is one of several involved in cortex formation (Bovetti et al., 2007; Stubbs et al., 2009). Analogously, neuroblast association with microvessels is a phenomenon that is nowadays widely accepted as one of the main drivers of the massive infiltration in human gliomas, proving that vessel sprouting and the mode of neuronal migration can be re-activated any time (Farin et al., 2006).

Interestingly is however that severe cortical disorganization is not invariably associated with aberrant vessel architecture or density, as shown in studies investigating the development of cortical microvasculature in *reeler* mice, exhibiting normal vasculature patterns and abnormal, inverted, laminar position of cortical neurons (Stubbs et al., 2009). Nevertheless the observation that newly formed neurons and glia cells strongly associate with the vascular plexus and are involved in migration processes suggest there is possible interaction between developing vasculature and cortex formation, which could have pathomechanistic significance (Stubbs et al., 2009).

In tubers, TSC1 or TSC2 gene dysfunction causes disinhibition of mTOR activity, which leads to upregulation of HIF-1a expression, increased vascular endothelial growth factor (VEGF) production and angiogenesis (El-Hashemite et al., 2003). Tubers are dynamic processes and serum VEGF levels in TSC patients are related to proliferation of

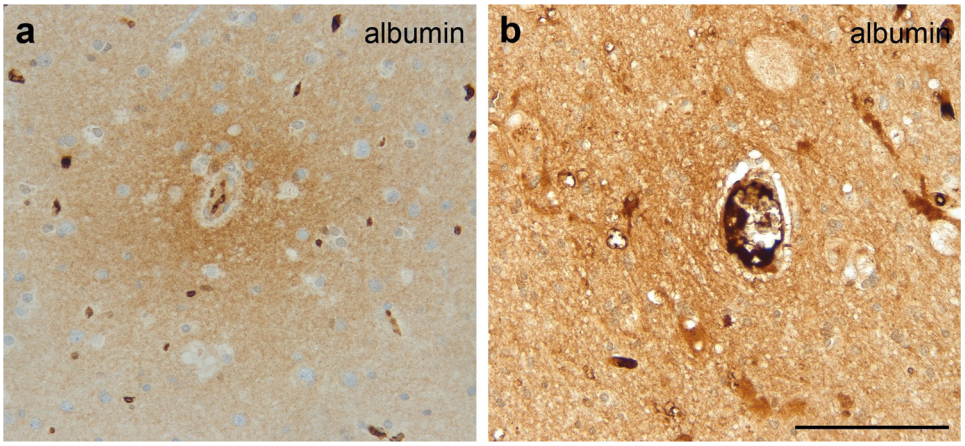

Fig. 5. Albumin deposits in TSC. **a** Deposits of albumin in grey matter indicating damage to the blood brain barrier. **B** similar deposits can be seen in white matter *Scale bar* in **b** = 100 μm and also applies to **a.**

lesions. VEGF production appears to be secondary to mTOR activation and is rapidly reversed by rapamycin, a mTOR inhibitor (Curatolo et al., 2018; El-Hashemite et al., 2003). This is also compatible with the observation of increasingly high vascular densities at older age.

BBB dysfunction is known to occur as a result of epileptic seizures and reciprocally plays a role in epileptogenesis and can sustain or aggravate epilepsy (van Vliet et al., 2015). Almost all TSC samples showed evidence of BBB dysfunction, with extravasation of albumin. In addition, there was an increase of T-cells that are not able to infiltrate the cortex and white matter without leakage of the BBB (van Horssen et al., 2012). However, we did not find a correlation between quantifications of microvascular density and BBB leakage.

Tubers exhibit complex activation of pro-inflammatory pathways, including chemokines, interleukin-1β, HMGB1 (high-mobility-group-box-1), TLR (toll-like-receptor), RAGE (receptors for advanced glycation end products) and complement mediated pathways (Curatolo et al., 2018). Local seizure activity triggers the release of a multitude of vasoactive substances which alter neurovascular coupling and can cause oxidative stress which both contribute to BBB dysfunction. In addition to promoting angiogenesis, VEGF increases BBB permeability through direct induction of inflammation (Gorter et al., 2015) and activation of matrix metalloproteases which break vessel walls and degrade tight junctions (Rigau et al., 2007). Alternatively, extravasated serum proteins are phagocytized by activated microglia and astrocytes (Alonso et al., 2011), elicit an inflammatory response (Ralay Ranaivo and Wainwright, 2010) and in turn possibly drive angiogenesis. In TSC samples we found a correlation between white matter vascular density and microglial activation, which co-occurred with T-cell activation. This supports a relation between inflammation and the observed angiogenesis.

Even though angiogenic processes and BBB dysfunction in epilepsy are generally considered detrimental for brain tissue and progression of disease, these could also be seen as protective mechanisms. Fast VEGF release, through FLK-1/AKT pathways, and activation of nitrous oxide-synthase, mediates vasodilation through nitrous oxide release (Ahmad et al., 2006; Papapetropoulos et al., 1997). In combination with increased vasculature these processes help to ensure adequate perfusion in tissue with increased metabolic demand due to epileptic activity.

We had hypothesized vascular density would be higher in lesional tissue compared to both control and perilesional samples due to processes related to epileptic activity and the underlying structural abnormality, and have no explanation for why we instead found no overall difference in vascular density between lesions and control samples, and lower perilesional vascular density.

Recent 7 T MRI studies showed an increased prominence of vascular structures co-localizing with cortical malformations in polymicrogyria (De Ciantis et al., 2015) and focal cortical dysplasia (Veersema et al., 2016). These vascular structures appeared to be mostly localized in the leptomeninges and sulci bordering the lesions. This was apparent on susceptibility-weighted contrast series, and therefore it could not be determined if this prominence was due to hemodynamic or structural changes, or a combination of both.

Unfortunately, it was not possible to examine leptomeningeal vasculature in the current study, since meninges were not sufficiently preserved in the surgical specimens.

Although in our study a significant increase vascular density in FCD lesions compared to normal controls could not be found, we did see an increase in vessel density in the FCD lesion compared to peri-lesional tissues. Our findings do not provide conclusive support there are vascular structural changes that could be the substrate of possible identifying or localizing imaging features of FCD. Hemodynamic and consequent blood oxygen level variations possibly better explain vascular prominence on T_2^* MR images.

ASL-MRI would have added valuable information regarding hemodynamic changes and possible correlation with vascular density and cytoarchitectural abnormalities, especially since prior studies showed conflicting results (Blauwblomme et al., 2014; Pollock et al., 2009; Wintermark et al., 2013). Unfortunately, ASL-MRI was not part of the standard pre-surgical diagnostic work-up and the retrospective nature of this study precluded collection of this data.

Sun et al. (Sun et al., 2018) observed fine vascular structures in white matter of tubers on 7 T susceptibility weighted images. This imaging feature is compatible with the findings if our study, and potentially could be of use in characterizing tubers. It remains to be clarified if this conveys information on epileptogenicity of individual tubers.

5. Conclusion

Cortical vascular density decreases with age in healthy controls, while it increases with age and with epilepsy duration in patients with epilepsy due to FCD or tubers in TSC. White matter vascular density was not correlated with age or epilepsy duration. In dysplasia and tubers lesional brain tissue showed higher vascular density compared to perilesional tissue. Compared to controls, we observed an increase in microvasculature in white matter of TSC cortical tubers, which was linked to an inflammatory response.

The increased white matter vascular density of tubers compared to FCD suggests that it is the underlying pathology, rather than seizure activity itself, that explains differences in vascular index. The lesional cortical vascular density increase with age and duration of epilepsy, however, appears to suggest a direct effect of ongoing epileptic activity.

Ethical statement

The study was approved by the institutional ethical committee and Biobank. We confirm that we have read the Journal's position on issues involved in ethical publication and affirm that this report is consistent with those guidelines.

Declaration of Competing Interest

None of the authors have any conflict of interest to disclose.

Acknowledgement

This work was supported by the Dutch Epilepsy Foundation (grant 12-12).

References

Ahmad, S., Hewett, P.W., Wang, P., Al-Ani, B., Cudmore, M., Fujisawa, T., Haigh, J.J., Le Noble, F., Wang, L., Mukhopadhyay, D., Ahmed, A., 2006. Direct evidence for endothelial vascular endothelial growth factor receptor-1 function in nitric oxide-mediated angiogenesis. Circ. Res. 99, 715–722. https://doi.org/10.1161/01.RES.0000243989.46006.b9.

Alonso, A., Reinz, E., Fatar, M., Hennerici, M.G., Meairs, S., 2011. Clearance of albumin following ultrasound-induced blood-brain barrier opening is mediated by glial but not neuronal cells. Brain Res. 1411, 9–16. https://doi.org/10.1016/j.brainres.2011.07.006.

Aronica, E., Mühlebner, A., 2017. Neuropathology of epilepsy. Handb. Clin. Neurol. 145, 193–216. https://doi.org/10.1016/B978-0-12-802395-2.00015-8.

Aronica, E., Ravizza, T., Zurolo, E., Vezzani, A., 2012. Astrocyte immune responses in epilepsy. Glia 60, 1258–1268. https://doi.org/10.1002/glia.22312.

Blauwblomme, T., Boddaert, N., Chémaly, N., Chiron, C., Pages, M., Varlet, P., Bourgeois, M., Bahi-Buisson, N., Kaminska, A., Grevent, D., Brunelle, F., Sainte-Rose, C., Archambaud, F., Nabbout, R., 2014. Arterial Spin Labeling MRI: a step forward in non-invasive delineation of focal cortical dysplasia in children. Epilepsy Res. 108, 1932–1939. https://doi.org/10.1016/j.eplepsyres.2014.09.029.

Blumcke, I., Spreafico, R., Haaker, G., Coras, R., Kobow, K., Bien, C.G., Pfäfflin, M., Elger, C., Widman, G., Schramm, J., Becker, A., Braun, K.P., Leijten, F., Baayen, J.C., Aronica, E., Chassoux, F., Hamer, H., Stefan, H., Rössler, K., Thom, M., Walker, M.C., Sisodiya, S.M., Duncan, J.S., McEvoy, A.W., Pieper, T., Holthausen, H., Kudernatsch, M., Meencke, H.J., Kahane, P., Schulze-Bonhage, A., Zentner, J., Heiland, D.H., Urbach, H., Steinhoff, B.J., Bast, T., Tassi, L., Lo Russo, G., Özkara, C., Oz, B., Krsek, P., Vogelgesang, S., Runge, U., Lerche, H., Weber, Y., Honavar, M., Pimentel, J., Arzimanoglou, A., Ulate-Campos, A., Noachtar, S., Hartl, E., Schijns, O., Guerrini, R., Barba, C., Jacques, T.S., Cross, J.H., Feucht, M., Mühlebner, A., Grunwald, T., Trinka,

E., Winkler, P.A., Gil-Nagel, A., Toledano Delgado, R., Mayer, T., Lutz, M., Zountsas, B., Garganis, K., Rosenow, F., Hermsen, A., von Oertzen, T.J., Diepgen, T.L., Avanzini, G., 2017. Histopathological findings in brain tissue obtained during epilepsy surgery. N. Engl. J. Med. 377, 1648–1656. https://doi.org/10.1056/NEJMoa1703784.

Blümcke, I., Thom, M., Aronica, E., Armstrong, D.D., Vinters, H.V., Palmini, A., Jacques, T.S., Avanzini, G., Barkovich, a J., Battaglia, G., Becker, A., Cepeda, C., Cendes, F., Colombo, N., Crino, P., Cross, J.H., Delalande, O., Dubeau, F., Duncan, J., Guerrini, R., Kahane, P., Mathern, G., Najm, I., Özkara, Ç., Raybaud, C., Represa, A., Roper, S.N., Salamon, N., Schulze-Bonhage, A., Tassi, L., Vezzani, A., Spreafico, R., 2011. The clinicopathologic spectrum of focal cortical dysplasias: a consensus classification proposed by an ad hoc Task Force of the ILAE Diagnostic Methods Commission. Epilepsia 52, 158–174. https://doi.org/10.1111/j.1528-1167.2010.02777.x.

Bovetti, S., Hsieh, Y.-C., Bovolin, P., Perroteau, I., Kazunori, T., Puche, A.C., 2007. Blood vessels form a scaffold for neuroblast migration in the adult olfactory bulb. J. Neurosci. 27, 5976–5980. https://doi.org/10.1523/JNEUROSCI.0678-07.2007.

Collins, C.E., Airey, D.C., Young, N.A., Leitch, D.B., Kaas, J.H., 2010. Neuron densities vary across and within cortical areas in primates. Proc. Natl. Acad. Sci. 107, 15927–15932. https://doi.org/10.1073/pnas.1010356107.

Coras, R., de Boer, O.J., Armstrong, D., Becker, A., Jacques, T.S., Miyata, H., Thom, M., Vinters, H.V., Spreafico, R., Oz, B., Marucci, G., Pimentel, J., Mühlebner, A., Zamecnik, J., Buccoliero, A.M., Rogerio, F., Streichenberger, N., Arai, N., Bugiani, M., Vogelgesang, S., Macaulay, R., Salon, C., Hans, V., Polivka, M., Giangaspero, F., Fauziah, D., Kim, J.-H., Liu, L., Dandan, W., Gao, J., Lindeboom, B., Blümcke, I., Aronica, E., 2012. Good interobserver and intraobserver agreement in the evaluation of the new ILAE classification of focal cortical dysplasias. Epilepsia 53, 1341–1348. https://doi.org/10.1111/j.1528-1167.2012.03508.x.

Curatolo, P., Moavero, R., van Scheppingen, J., Aronica, E., 2018. mTOR dysregulation and tuberous sclerosis-related epilepsy. Expert Rev. Neurother. 18, 185–201. https://doi.org/10.1080/14737175.2018.1428562.

De Ciantis, A., Barkovich, A.J., Cosottini, M., Barba, C., Montanaro, D., Costagli, M., Tosetti, M., Biagi, L., Dobyns, W.B., Guerrini, R., 2015. Ultra-high-field MR imaging in polymicrogyria and epilepsy. Am. J. Neuroradiol. 36, 309–316. https://doi.org/10.3174/ajnr.A4116.

El-Hashemite, N., Walker, V., Zhang, H., Kwiatkowski, D.J., 2003. Loss of Tsc1 or Tsc2 induces vascular endothelial growth factor production through mammalian target of rapamycin. Cancer Res. 63, 5173–5177.

Englot, D.J., Berger, M.S., Barbaro, N.M., Chang, E.F., 2012. Factors associated with seizure freedom in the surgical resection of glioneuronal tumors. Epilepsia 53, 51–57. https://doi.org/10.1111/j.1528-1167.2011.03269.x.

Farin, A., Suzuki, S.O., Weiker, M., Goldman, J.E., Bruce, J.N., Canoll, P., 2006. Transplanted glioma cells migrate and proliferate on host brain vasculature: a dynamic analysis. Glia 53, 799–808. https://doi.org/10.1002/glia.20334.

Gorter, J.A., Van Vliet, E.A., Aronica, E., 2015. Status epilepticus, blood-brain barrier disruption, inflammation, and epileptogenesis. Epilepsy Behav. 49, 13–16. https://doi.org/10.1016/j.yebeh.2015.04.047.

Ishi, K., Sasaki, M., Kitagaki, H., Sakamoto, S., Yamaji, S., Maeda, K., 1996. Regional difference in cerebral blood flow and oxidative metabolism in human cortex. J. Nucl. Med. 37, 1086–1088.

Liang, S., Zhang, Juncheng, Yang, Z., Zhang, S., Cui, Z., Cui, J., Zhang, Jiwu, Liu, N., Ding, P., 2017. Long-term outcomes of epilepsy surgery in tuberous sclerosis complex. J. Neurol. 264, 1146–1154. https://doi.org/10.1007/s00415-017-8507-y.

Marín-Padilla, M., 2012. The human brain intracerebral microvascular system: development and structure. Front. Neuroanat. 6, 38. https://doi.org/10.3389/fnana.2012.00038.

Mito, T., Konomi, H., Houdou, S., Takashima, S., 1991. Immunohistochemical study of the vasculature in the developing brain. Pediatr. Neurol. 7, 18–22. https://doi.org/10.1016/0887-8994(91)90100-Y.

Mühlebner, A., Van Scheppingen, J., Hulshof, H.M., Scholl, T., Iyer, A.M., Anink, J.J., Nellist, M.D., Jansen, F.E., Spliet, W.G.M., Krsek, P., Benova, B., Zamecnik, J., Crino, P.B., Prayer, D., Czech, T., Wöhrer, A., Rahimi, J., Höftberger, R., Hainfellner, J.A., Feucht, M., Aronica, E., 2016. Novel histopathological patterns in cortical tubers of epilepsy surgery patients with tuberous sclerosis complex. PLoS One 11, 1–15. https://doi.org/10.1371/journal.pone.0157396.

Northrup, H., Krueger, D.A., International Tuberous Sclerosis Complex Consensus Group, 2013. Tuberous sclerosis complex diagnostic criteria update: recommendations of the 2012 International Tuberous Sclerosis Complex Consensus Conference. Pediatr. Neurol. 49, 243–254. https://doi.org/10.1016/j.pediatrneurol.2013.08.001.

Palmini, A., Najm, I., Avanzini, G., Babb, T., Guerrini, R., Foldvary-Schaefer, N., Jackson, G., Lüders, H.O., Prayson, R., Spreafico, R., Vinters, H.V., 2004. Terminology and classification of the cortical dysplasias. Neurology 62, S2–8.

Papapetropoulos, A., García-Cardeña, G., Madri, J.A., Sessa, W.C., 1997. Nitric oxide production contributes to the angiogenic properties of vascular endothelial growth factor in human endothelial cells. J. Clin. Invest. 100, 3131–3139. https://doi.org/10.1172/JCI119868.

Pollock, J.M., Whitlow, C.T., Tan, H., Kraft, R., Burdette, J.H., Maldjian, J., 2009. Pulsed arterial spin-labeled MR imaging evaluation of tuberous sclerosis. AJNR Am. J. Neuroradiol. 30, 815–820. https://doi.org/10.3174/ajnr.A1428.

Prabowo, A.S., Iyer, A.M., Anink, J.J., Spliet, W.G.M., van Rijen, P.C., Aronica, E., 2013. Differential expression of major histocompatibility complex class I in developmental glioneuronal lesions. J. Neuroinflammation 10, 12. https://doi.org/10.1186/1742-2094-10-12.

Ralay Ranaivo, H., Wainwright, M.S., 2010. Albumin activates astrocytes and microglia through mitogen-activated protein kinase pathways. Brain Res. 1313, 222–231. https://doi.org/10.1016/j.brainres.2009.11.063.

Riddle, D.R., Sonntag, W.E., Lichtenwalner, R.J., 2003. Microvascular plasticity in aging. Ageing Res. Rev. 2, 149–168. https://doi.org/10.1016/S1568-1637(02)00064-8.

Rigau, V., Morin, M., Rousset, M.-C., de Bock, F., Lebrun, A., Coubes, P., Picot, M.-C., Baldy-Moulinier, M., Bockaert, J., Crespel, A., Lerner-Natoli, M., 2007. Angiogenesis is associated with blood-brain barrier permeability in temporal lobe epilepsy. Brain 130, 1942–1956. https://doi.org/10.1093/brain/awm118.

Rockel, A.J., Hiorns, R.W., Powell, T.P.S., 1980. The Basic Uniformity in Structure of the Neocortex. Brain 103, 221–244. https://doi.org/10.1093/brain/103.2.221.

Scholl, T., Mühlebner, A., Ricken, G., Gruber, V., Fabing, A., Samueli, S., Gröppel, G., Dorfer, C., Czech, T., Hainfellner, J.A., Prabowo, A.S., Reinten, R.J., Hoogendijk, L., Anink, J.J., Aronica, E., Feucht, M., 2017. Impaired oligodendroglial turnover is associated with myelin pathology in focal cortical dysplasia and tuberous sclerosis complex. Brain Pathol. 27, 770–780. https://doi.org/10.1111/bpa.12452.

Skoglund, T.S., Pascher, R., Berthold, C.H., 1996. Heterogeneity in the columnar number of neurons in different neocortical areas in the rat. Neurosci. Lett. 208, 97–100. https://doi.org/10.1016/0304-3940(96)12569-6.

Stubbs, D., DeProto, J., Nie, K., Englund, C., Mahmud, I., Hevner, R., Molnár, Z., 2009. Neurovascular congruence during cerebral cortical development. Cereb. Cortex 19 (Suppl 1), i32–41. https://doi.org/10.1093/cercor/bhp040.

Sun, K., Cui, J., Wang, B., Jiang, T., Chen, Z., Cong, F., Zhuo, Y., Liang, S., Xue, R., Yu, X., Chen, L., 2018. Magnetic resonance imaging of tuberous sclerosis complex with or without epilepsy at 7 T. Neuroradiology 60, 785–794. https://doi.org/10.1007/s00234-018-2040-2.

van Horssen, J., Singh, S., van der Pol, S., Kipp, M., Lim, J.L., Peferoen, L., Gerritsen, W., Kooi, E.-J., Witte, M.E., Geurts, J.J.G., de Vries, H.E., Peferoen-Baert, R., van den Elsen, P.J., van der Valk, P., Amor, S., 2012. Clusters of activated microglia in normal-appearing white matter show signs of innate immune activation. J. Neuroinflammation 9, 156. https://doi.org/10.1186/1742-2094-9-156.

van Vliet, E.A., Aronica, E., Gorter, J.A., 2015. Blood-brain barrier dysfunction, seizures and epilepsy. Semin. Cell Dev. Biol. 38, 26–34. https://doi.org/10.1016/j.semcdb.2014.10.003.

Veersema, T.J., Swampillai, B., Ferrier, C.H., Eijsden, P., Gosselaar, P.H., van Rijen, P.C., Spliet, W.G.M., Mühlebner, A., Aronica, E., Braun, K.P.J., 2019. Long-term seizure outcome after epilepsy surgery in patients with mild malformation of cortical development and focal cortical dysplasia. Epilepsia Open 4, 170–175. https://doi.org/10.1002/epi4.12289.

Veersema, T.J., van Eijsden, P., Gosselaar, P.H., Hendrikse, J., Zwanenburg, J.J.M., Spliet, W.G.M., Aronica, E., Braun, K.P.J., Ferrier, C.H., 2016. 7 tesla T2*-weighted MRI as a tool to improve detection of focal cortical dysplasia. Epileptic Disord. 18, 315–323. https://doi.org/10.1684/epd.2016.0838.

Wintermark, P., Lechpammer, M., Warfield, S.K., Kosaras, B., Takeoka, M., Poduri, A., Madsen, J.R., Bergin, A.M., Whalen, S., Jensen, F.E., 2013. Perfusion imaging of focal cortical dysplasia using arterial spin labeling: correlation with histopathological vascular density. J. Child Neurol. 28, 1474–1482. https://doi.org/10.1177/0883073813488666.

Wong-Riley, M.T.T., 2010. Energy metabolism of the visual system. Eye Brain 2, 99–116. https://doi.org/10.2147/EB.S9078.

Young, N.A., Collins, C.E., Kaas, J.H., 2013. Cell and neuron densities in the primary motor cortex of primates. Front. Neural Circuits 7, 1–11. https://doi.org/10.3389/fncir.2013.00030.